Supramolecular Architectonics with Carbon Nanoclusters

A host-guest interaction between fullerenes and cyclic dimers of metalloporphyrins results in the formation of doubly layered π-electronic supramolecules, whose thermodynamic stability and dynamics in guest exchange can be tuned by the selection of the metal ions at the outer porphyrin layer. In particular, the host molecule with rhodium ions exhibits an extremely high affinity toward fullerenes.

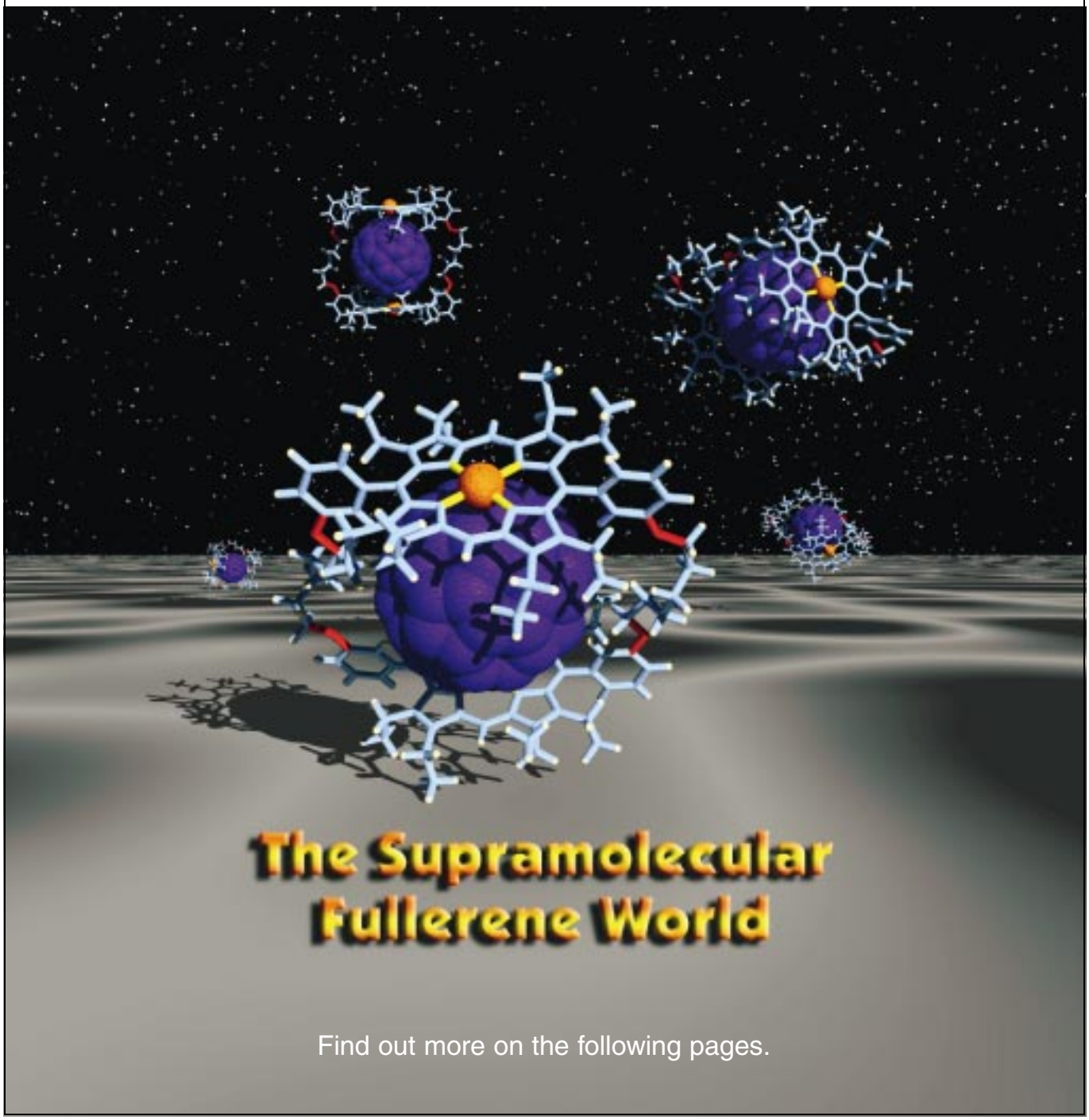

  1433-7851/01/4010-1857 $ 17.50+.50/0

Cyclic Dimers of Metalloporphyrins as Tunable Hosts for Fullerenes: A Remarkable Effect of Rhodium(III)**

Jian-Yu Zheng, Kentaro Tashiro, Yusuke Hirabayashi, Kazushi Kinbara, Kazuhiko Saigo,* Takuzo Aida,* Shigeru Sakamoto, and Kentaro Yamaguchi

With regard to multiwalled graphitic nanoparticles such as carbon nanopolyhedrons,[1] nanocapsules,[2] and buckyonions,[3] wrapping of fullerenes in large π-conjugated molecular envelopes is an interesting subject, which may extend the π-electronic conjugation of fullerenes in a three-dimensional fashion. Recently, we found that a cyclic dimer of zinc porphyrin (**1**-Zn) forms an inclusion complex with C_{60} (**1**-Zn ⊃ C_{60}), of which the association constant K_{assoc} of $6.7 \times 10^5\,M^{-1}$ is the highest value reported to date in organic media.[4] This finding prompted us to investigate whether the central metal ions play an essential role in this supramolecular interaction.[5] Here we report the results of a study on the interaction of fullerenes such as C_{60} and C_{70} with a series of metalloporphyrin cyclic dimers (**1**-M; M = 2H, Co, RhMe, Ni, Cu, Ag, and Zn), with emphasis on the extremely high affinity of the host molecule for Group 9 metal ions such as rhodium(III).[6]

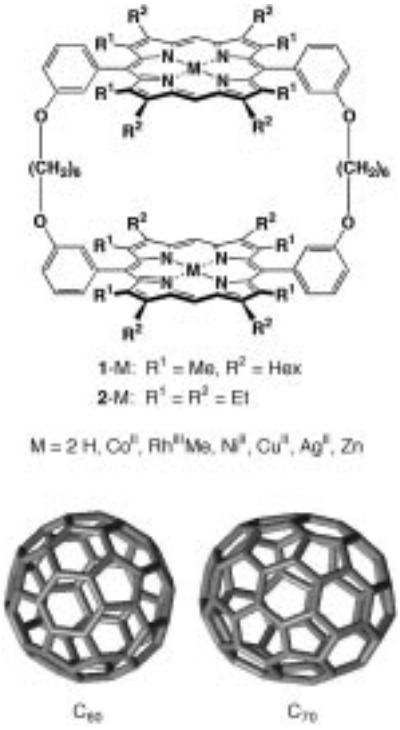

X-ray crystallography is informative of fullerene–metalloporphyrin interactions.[7] By slow diffusion of acetonitrile into a CH_2Cl_2 solution of a mixture of C_{60} and **2**-Zn, a black prismatic crystal of a 1:1 complex of C_{60} with **2**-Zn, appropriate for X-ray crystallography, was obtained.[8] Figure 1 shows an ORTEP plot of the complex at −110 °C,[9] where **2**-Zn in the crystal adopts a C_i-symmetric conformation, the inversion center of which is shared with that of included C_{60}. The hexamethylene linkers of **2**-Zn are folded to adjust the porphyrin–porphyrin distance, and the porphyrin macrocycles are slightly distorted from planarity so as to accommodate the convex shape of C_{60}. One of the 5:6 ring-juncture C–C bonds of C_{60} is located on the central metal ion. The distances between the zinc atom and these two unique carbon atoms are 2.765(9) and 2.918(10) Å, which are clearly shorter than the sum of the van der Waals radii (3.09 Å).[10] Furthermore, the distances between the pyrrole α-C atoms of the porphyrin moieties and three proximal carbon atoms of C_{60} (3.320–3.346 Å) are slightly but definitely shorter than the typical interlayer distance of graphite (3.354 Å).[11] These observations suggest the presence of a π interaction between

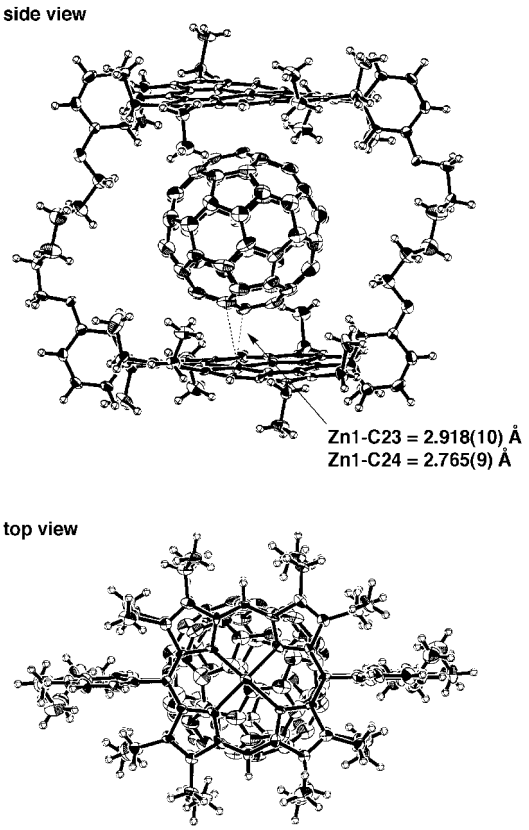

Figure 1. ORTEP plot of an inclusion complex of C_{60} with **2**-Zn (**2**-Zn ⊃ C_{60}).

[*] Prof. Dr. T. Aida, Dr. K. Tashiro, Y. Hirabayashi
Department of Chemistry and Biotechnology
Graduate School of Engineering, The University of Tokyo
7-3-1 Hongo, Bunkyo-ku, Tokyo 113-8656 (Japan)
Fax: (+81) 3-5841-7310
E-mail: aida@macro.t.u-tokyo.ac.jp
Prof. Dr. K. Saigo, Dr. J.-Y. Zheng, Dr. K. Kinbara
Department of Integrated Biosciences
Graduate School of Frontier Sciences, The University of Tokyo
7-3-1 Hongo, Bunkyo-ku, Tokyo 113-8656 (Japan)
Fax: (+81) 3-5802-3348
E-mail: saigo@chiral.t.u-tokyo.ac.jp
S. Sakamoto, Prof. Dr. K. Yamaguchi
(Responsible for X-ray crystallography)
Chemical Analysis Center, Chiba University
Yayoi-cho, Inage-ku, Chiba 263-8522 (Japan)

[**] We thank Dr. F. Hasegawa of the Science University of Tokyo for HR-MS measurements. J.-Y.Z. and K.S. thank the JSPS for financial support.

Supporting information for this article is available on the WWW under http://www.angewandte.com or from the author.

  1433-7851/01/4010-1858 $ 17.50+.50/0

the zinc porphyrin moieties and the included fullerene in the solid state.[7]

Similarly to our previous study,[4] we conducted spectroscopic titration of the metalloporphyrin cyclic dimers bearing Group 9–11 metal ions (**1**-M; M = Co, Ni, Cu, Ag) in addition to free-base **1**-2H, with C_{60} in benzene at 25 °C, in which the Soret absorption band of each host molecule showed a clear red shift with a decrease in absorbance.[12] From the observed spectral change profiles, the association constants K_{assoc} were evaluated as shown in Figure 2a, whereby K_{assoc} of **1**-2H is

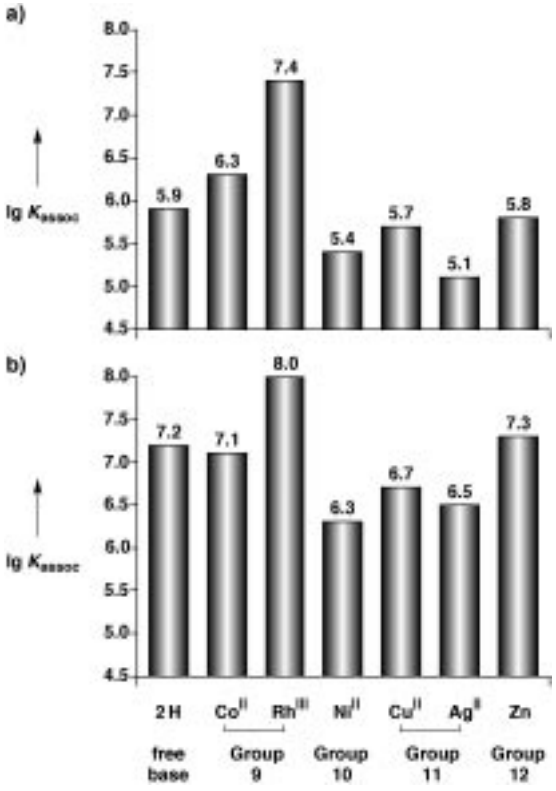

Figure 2. Association constants K_{assoc} of metalloporphyrin cyclic dimers **1**-M with C_{60} (a) and C_{70} (b) in benzene at 25 °C.

comparable to that of **1**-Zn,[4] while **1**-Ni, **1**-Cu, and **1**-Ag with Group 10 and 11 metal ions are inferior to these two host molecules. On the other hand, a host molecule with Group 9 metal ions such as **1**-Co is clearly superior to all these host molecules. Therefore, we synthesized **1**-RhMe with rhodium(III) ions at the porphyrin center. Interestingly, the K_{assoc} value of **1**-RhMe with C_{60} ($2.4 \times 10^7\,M^{-1}$) was even higher than that of **1**-Co.[13] For the interaction with C_{70}, the affinities of the cyclic host molecules **1**-M displayed essentially the same dependency on the central metal ion as in Figure 2a, whereby the observed K_{assoc} values were nearly or more than one order of magnitude larger than those with C_{60} (Figure 2b). In particular, **1**-RhMe again exhibited an extremely high affinity; the K_{assoc} value of about $10^8\,M^{-1}$ apparently exceeds the experimental upper limit of accuracy for the spectroscopic titration. The K_{assoc} values of **1**-2H, **1**-Co, and **1**-Zn were also greater than $10^7\,M^{-1}$, whereas the other three host molecules with Group 10 and 11 metal ions (**1**-Ni, **1**-Cu, and **1**-Ag) were inferior to the above host molecules ($K_{assoc} < 10^7\,M^{-1}$). With respect to the extremely high affinity of **1**-RhMe toward fullerenes, the inclusion complex **1**-RhMe ⊃ C_{60} eluted as a single component not only in GPC on Polystyragel ($CHCl_3$) but also in HPLC on Buckyprep (toluene), while other complexes such as **1**-Zn ⊃ C_{60}, in contrast, dissociated completely under the same chromatographic conditions.

For the interaction of **1**-RhMe with fullerenes, the axial methyl groups of the host serve as an NMR probe: the ^1H NMR spectrum of **1**-RhMe alone in C_6D_6 at 25 °C showed eight inequivalent doublets assigned to MeRh at $\delta = -5.15$, -5.30, -5.36, -5.67, -5.77, -5.79, -5.84, and -5.85, which indicate the presence of several conformational isomers.[4] When C_{60} was added to this solution, **1**-RhMe underwent a conformational change to give only a single doublet for MeRh (**1**-RhMe ⊃ C_{60}) at $\delta = -5.06$. In the ^{13}C NMR spectrum in $CDCl_3$, **1**-RhMe ⊃ C_{60} showed a signal assigned to MeRh in a region downfield (d, $\delta = -6.9$, $\Delta\delta = 6.9$) from that of **1**-RhMe ($\delta = -13.8$), while included C_{60} displayed a signal in a region upfield ($\delta = 139.4$; $\Delta = -3.6$) from that of free C_{60} ($\delta = 143.0$). In contrast, upon coordination of an electron-donating ligand such as bipyridine (bpy) to **1**-RhMe (**1**-RhMe ⊃ bpy), the ^{13}C NMR signal for MeRh shifted upfield[14] to $\delta = -16.0$ ($\Delta\delta = -2.2$). Therefore, it is likely that **1**-RhMe ⊃ C_{60} involves a rhodium-to-fullerene charge transfer interaction.

The much higher affinities of the host molecules toward C_{70} than C_{60} are considered to be a result of the ovality of C_{70} (7.1/7.9 Å). Because of this elliptical shape, C_{70} itself shows five inequivalent ^{13}C NMR signals.[15, 16] When ^{13}C-enriched C_{70} was mixed with **1**-Zn in $CDCl_3/CS_2$ (1:1), all the C_{70} signals shifted upfield, whereby the change in chemical shift was more pronounced for the equatorial carbon atoms than for those at the pole over a wide temperature range ($\Delta\delta_{equator} = -3.8$, $\Delta\delta_{pole} = -2.4$ at 25 °C; $\Delta\delta_{equator} = -4.1$, $\Delta\delta_{pole} = -2.5$ at -60 °C).[5, 17] Since the upfield shifts of the fullerene signals are induced mostly by the shielding effect of the porphyrin macrocycle, this trend indicates that included C_{70} adopts a side-on conformation with respect to the two zinc porphyrins, which possibly maximizes the host–guest π interaction.[5, 7b] With **1**-RhMe as host, C_{70} upon inclusion showed a similar change in spectral profile at 25 °C ($\Delta\delta_{equator} = -3.6$, $\Delta\delta_{pole} = -3.0$).[18] However, on lowering the temperature to -60 °C, the shielding effect became slightly but definitely more pronounced for the carbon atoms at the pole than for those on the equator ($\Delta\delta_{equator} = -3.9$, $\Delta\delta_{pole} = -4.1$), which suggests that an end-on orientation is preferred for included C_{70} at low temperatures.[19]

Variable-temperature (VT) ^{13}C NMR spectroscopy is informative of the dynamics of the complexation of fullerenes with cyclic dimers of metalloporphyrins.[5] For example, a 1:2 mixture of **1**-Zn and ^{13}C-enriched C_{60} at -60 °C in [D_8]toluene showed two singlet ^{13}C NMR signals at $\delta = 139.7$ and 142.9 arising from included and free C_{60} molecules, respectively (Figure 3a). On elevation of the temperature, the signals coalesced at 20 °C as a result of exchange of C_{60} faster than the NMR timescale. When ^{13}C-enriched C_{70} was the guest ([**1**-Zn]/[C_{70}] = 1:2), a similar coalescence signature was observed at a higher temperature (60 °C), as the K_{assoc} value for C_{70} is 31 times larger than that for C_{60}. In sharp contrast, although the K_{assoc} value is almost comparable to that for the **1**-Zn/C_{70}

  1433-7851/01/4010-1859 $ 17.50+.50/0

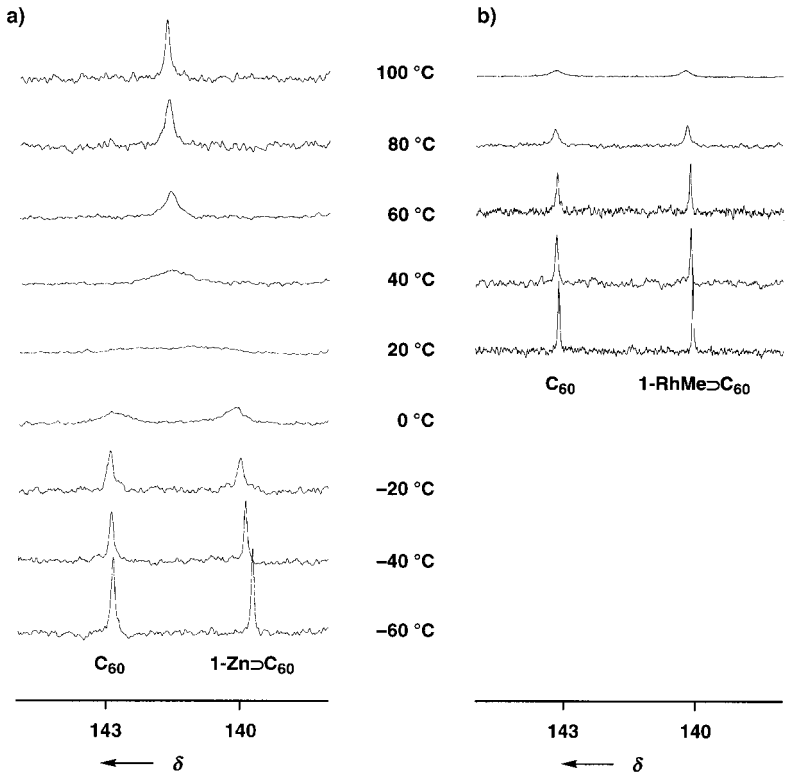

Figure 3. VT ^{13}C NMR profiles of ^{13}C-enriched C_{60} in the presence of 0.5 equiv of **1**-Zn (a) and **1**-RhMe (b) in [D_8]toluene.

system (Figure 2), the **1**-RhMe/C_{60} (1:2) system did not show such a coalescence phenomenon even at 100 °C (Figure 3b). The same was true of the **1**-RhMe/C_{70} system. Since the rate constant of dissociation k_{dissoc} is much smaller than that of association k_{assoc} ($K_{assoc} = k_{assoc}/k_{dissoc} \gg 1$), the above coalescence profiles should reflect the magnitude of k_{dissoc} rather than k_{assoc}. From the differences in resonance frequency between the free and included fullerenes,[20] the k_{dissoc} values for **1**-Zn ⊃ C_{60} and **1**-Zn ⊃ C_{70} at the coalescence temperatures were estimated to be 450 (20 °C) and 310 s^{-1}[21] (60 °C), respectively.[22] The absence of coalescence for the **1**-RhMe/fullerene systems indicates that **1**-RhMe ⊃ fullerenes dissociate much less frequently than **1**-Zn ⊃ fullerenes. Together with the fact that rhodium(III) porphyrins can form ethene π complexes,[23] the very low dissociation activities of **1**-RhMe ⊃ fullerenes suggest some sort of bonding interaction between the central rhodium(III) ions of the host and the included fullerenes.

By taking advantage of the tunable affinity of the host molecule toward fullerenes, choice of appropriate central metal ions of the host allows simple separation of C_{70} from a mixture of C_{60} and C_{70}. For example, a C_{60}/C_{70} mixture containing 65% of C_{70} was mixed with **2**-Zn ([fullerenes]/[**2**-Zn] = 10) in benzene,[24] and the inclusion complexes were isolated by column chromatography on alumina, and then treated with 4,4′-bipyridine to extract the included fullerenes from the cavity. According to HPLC analysis on Buckyprep with toluene as eluent, the extract contained almost pure C_{70} (>99%). Even from a C_{60}/C_{70} mixture with a much lower C_{70} content such as 20%, an extract highly enriched in C_{70} (91%) was again obtained.

In conclusion, we have demonstrated a remarkable effect of the central metal ions on the interaction of metalloporphyrin cyclic dimers with fullerenes. In particular, the extremely high association constants ($\sim 10^8\ M^{-1}$)[25] and low dissociation activities of the **1**-RhMe/fullerene systems should allow construction of more complex supramolecular architectures based on fullerenes. Further studies along this line together with an investigation of electronic and magnetic properties of such multiwalled π-electron supramolecular systems are now in progress.

Received: January 2, 2001 [Z16351]

[1] T. W. Ebbesen, P. M. Ajayan, *Nature* **1992**, *358*, 220.
[2] a) R. S. Ruoff, D. C. Lorents, B. Chan, R. Malhotra, S. Subramoney, *Science* **1993**, *259*, 346; b) M. Tomita, Y. Saito, T. Hayashi, *Jpn. J. Appl. Phys.* **1993**, *32*, L280.
[3] D. Ugarte, *Nature* **1992**, *359*, 707.
[4] K. Tashiro, T. Aida, J.-Y. Zheng, K. Kinbara, K. Saigo, S. Sakamoto, K. Yamaguchi, *J. Am. Chem. Soc.* **1999**, *121*, 9477.
[5] For a more recent example of a supramolecular interaction of fullerenes with porphyrins, see D. Sun, F. S. Tham, C. A. Reed, L. Chaker, M. Burgess, P. D. W. Boyd, *J. Am. Chem. Soc.* **2000**, *122*, 10704.
[6] For experimental details, see Supporting Information.
[7] a) M. M. Olmstead, D. A. Costa, K. Maitra, B. C. Noll, S. L. Phillips, P. M. van Calcar, A. L. Balch, *J. Am. Chem. Soc.* **1999**, *121*, 7090; b) P. D. W. Boyd, M. C. Hodgson, C. E. F. Rickard, A. G. Oliver, L. Chaker, P. J. Brothers, R. D. Bolskar, F. S. Tham, C. A. Reed, *J. Am. Chem. Soc.* **1999**, *121*, 10487; c) T. Ishii, N. Aizawa, M. Yamashita, H. Matsuzaka, T. Kodama, K. Kikuchi, I. Ikemoto, Y. Isawa, *J. Chem. Soc. Dalton Trans.* **2000**, 4407.
[8] Crystal data for **2**-Zn ⊃ C_{60} ($C_{168}H_{124}O_4N_8Zn_2$): crystal dimensions $0.80 \times 0.30 \times 0.18$ mm^3, triclinic, space group $P\bar{1}$, $a = 13.6550(11)$, $b = 15.3346(12)$, $c = 16.2865(13)$ Å, $\alpha = 108.187(2)$, $\beta = 107.904(2)$, $\gamma = 97.732(3)°$, $V = 2957.7(4)$ Å^3, $Z = 1$, $\rho_{calcd} = 1.38$ g cm^{-3}, $\mu(Mo_{K\alpha}) = 4.74$ cm^{-1}, $F(000) = 1280$, $2\Theta_{max} = 49.4°$, $T = 163$ K, ω scans, 16875 reflections measured, 9965 unique, 4609 with $I > 3.0\sigma(I)$, 883 variables, $R = 0.075$, $Rw = 0.087$, $S = 2.09$, $(\Delta/\sigma)_{max} = 0.83$, $\rho_{max} = 1.06$ e$^-$ Å^{-3}, $\rho_{min} = -1.14$ e Å^{-3}. Data were collected on a Bruker SMART 1000 CCD diffractometer with monochromated $Mo_{K\alpha}$ radiation ($\lambda = 0.7101$ Å) using SAINT (Siemens) for cell refinement and data reduction. Absorption correction was not applied. The crystal structure was solved by using SIR97 and refined on F by the full-matrix least-squares method included in TEXSAN, version 1.1 (Molecular Structure Co.). Non-hydrogen atoms were refined anisotropically. All H atoms with isotropic thermal parameters were located on the calculated positions (not refined). Crystallographic data (excluding structure factors) for the structures reported in this paper have been deposited with the Cambridge Crystallographic Data Centre as supplementary publication no. CCDC-150074. Copies of the data can be obtained free of charge on application to CCDC, 12 Union Road, Cambridge CB21EZ, UK (fax: (+44) 1223-336-033; e-mail: deposit@ccdc.cam.ac.uk).
[9] At room temperature, the crystal structure showed only an electron density within the cavity of **2**-Zn; this suggests that included C_{60} rotates in the solid state.
[10] A. Bondi, *J. Phys. Chem.* **1964**, *68*, 441.
[11] R. E. Franklin, *Acta Crystallogr.* **1951**, *4*, 253.
[12] Similar red shifts in the Soret region have been reported for covalently linked porphyrin/C_{60} diads: N. Armaroli, G. Marconi, L. Echegoyen, J.-P. Bourgeois, F. Diederich, *Chem. Eur. J.* **2000**, *6*, 1629.
[13] The superiority of **1**-RhMe for the inclusion of C_{60} was also confirmed in 1,2,4-trichlorobenzene, a better solvent for fullerenes than benzene, in which the observed K_{assoc} value of $6.8 \times 10^5\ M^{-1}$ was again much

  1433-7851/01/4010-1860 $ 17.50+.50/0

higher than those of **1**-Zn ($1.4 \times 10^4\,M^{-1}$) and **1**-Co ($7.2 \times 10^4\,M^{-1}$) under the same conditions.

[14] ^{13}C NMR ($CDCl_3$, 25 °C) of bipyridine: $\delta = 150.3$ (C2), 121.1 (C3), 145.2 (C4); **1**-RhMe ⊃ bipyridine: $\delta = 144.2$ (C2), 117.9 (C3), 140.7 (C4).

[15] ^{13}C NMR ($CDCl_3/CS_2$ 1:1): C_{70} (equator to pole) at 25 °C: $\delta = 130.4$, 144.9, 147.6, 146.9, 150.1; at −60 °C: $\delta = 130.0$, 144.5, 147.2, 146.5, 149.7; C_{70}/**1**-Zn (1:2) at 25 °C: $\delta = 126.6$ ($\Delta\delta = -3.8$), 141.3 (−3.6), 144.5 (−3.1), 144.2 (−2.7), 147.7 (−2.4); at −60 °C: $\delta = 125.9$ ($\Delta\delta = -4.1$), 140.7 (−3.8), 143.9 (−3.3), 143.7 (−2.8), 147.2 (−2.5).

[16] R. Taylor, J. P. Hare, A. K. Abdul-Sada, H. W. Kroto, *J. Chem. Soc. Chem. Commun.* **1990**, 1423.

[17] T. Haino, M. Yanase, Y. Fukazawa, *Angew. Chem.* **1998**, *110*, 1044; *Angew. Chem. Int. Ed.* **1998**, *37*, 997.

[18] ^{13}C NMR ($CDCl_3/CS_2$ 1:1) of C_{70}/**1**-RhMe (1:2) (equator to pole) at 25 °C: $\delta = 126.8$ ($\Delta\delta = -3.6$), 141.2 (−3.7), 144.2 (−3.4), 143.8 (−3.1), 147.1 (−3.0); at −60 °C: $\delta = 126.5$ ($\Delta\delta = -3.9$), 141.0 (−3.9), 143.6 (−4.0), 142.7 (−4.2), 146.0 (−4.1).

[19] Selective coordination of Pt^0 and Ir^I to C_{70} at 6:6 ring junctions close to the pole has been reported: a) A. L. Balch, V. J. Catalano, J. W. Lee, M. M. Olmstead, S. R. Parkin, *J. Am. Chem. Soc.* **1991**, *113*, 8953; b) A. L. Balch, L. Hao, M. M. Olmstead, *Angew. Chem.* **1996**, *108*, 211; *Angew. Chem. Int. Ed. Engl.* **1996**, *35*, 188.

[20] Chemical shifts of C_{60} and C_{70} at 20 and 60 °C, respectively, in the presence of excess amounts of **1**-Zn (C_{60}/**1**-Zn = 1:5, C_{70}/**1**-Zn = 1:2.4) were used.

[21] Estimated on the basis of the coalescence profile of a ^{13}C NMR signal of the carbon atoms on the pole of C_{70}.

[22] J. K. M. Sanders, B. K. Hunter, *Modern NMR Spectroscopy*, Oxford University Press, Oxford, **1987**.

[23] a) B. Wayland, S. L. Van Voorhees, K. J. Del Rossi, *J. Am. Chem. Soc.* **1987**, *109*, 6513; b) J. L. Maxwell, K. C. Brown, D. W. Bartley, T. Kodadek, *Science* **1992**, *256*, 1544.

[24] $K_{assoc} = 1.4 \times 10^6\,M^{-1}$ for C_{60} and $2.4 \times 10^7\,M^{-1}$ for C_{70} in benzene at 25 °C.

[25] Almost comparable to the association constant of a quadruple hydrogen bonding interaction, usable for the construction of supramolecular polymers: B. J. B. Folmer, R. P. Sijbesma, H. Kooijman, A. L. Spek, E. M. Meijer, *J. Am. Chem. Soc.* **1999**, *121*, 9001.

Photoelectrochemistry with Controlled DNA-Cross-Linked CdS Nanoparticle Arrays**

Itamar Willner,* Fernando Patolsky, and Julian Wasserman

Electronics based on DNA has been the subject of extensive recent research activities that address the conductivity features of double-stranded (ds) DNA,[1–7] the use of ds-DNA as a template for the construction of nanowires,[8] and the employment of metal nanoparticles cross-linked by DNA as single-electron charging devices.[9, 10] The optical properties of DNA-cross-linked Au nanoparticles were recently studied and applied for DNA sensing,[11, 12] and nanoarchitectures of DNA/Au nanoparticles were assembled.[13] The electronic transduction of DNA sensing and, in particular, amplified DNA analyses were recently studied by using electrochemical measurements[14–23] or microgravimetry[16] with a quartz-crystal microbalance. Direct electrochemical detection of DNA was achieved by monitoring the electrochemical response of DNA[14–16] or by the incorporation of redox-labels into ds-DNA.[17–19] The amplified detection of DNA was accomplished by the use of biocatalytic conjugates[20, 21] and the application of labeled liposomes[22, 23] or nanoparticles.[24, 25]

Herein we describe the novel architecture of double-stranded DNA-cross-linked CdS nanoparticle arrays on electrode supports and the structurally controlled generation of photocurrents upon irradiation of these arrays. The electrostatic binding of $[Ru(NH_3)_6]^{3+}$ to the ds-DNA units provides tunneling routes for the conduction-band electrons and thus results in enhanced photocurrents. Besides the unique and novel photoelectrochemical features of the systems, the assemblies provide a new means for the optical fluorescence and electronic (photoelectrochemical) transduction of DNA-sensing events.

CdS nanoparticles (2.6 ± 0.4 nm) were functionalized with thiolated oligonucleotide **1** or **2**. These two oligonucleotides are complementary to the 5′- and 3′-ends of the target DNA **3**. The size of the CdS nanoparticles was determined from HR-transmission electron microscopy (TEM) images (average of 150 particles). Using the absorption spectra of the CdS nanoparticles ($\lambda_{max} = 405$ nm) and the Brus equation[26] gave a similar particle size. We estimate that about 20–24 oligonucleotide units are associated with each CdS nanoparticle (see *Experimental Section* for details). Figure 1 shows the stepwise assembly of the DNA-cross-linked CdS particles on an Au electrode. The oligonucleotide **1** was assembled on the Au electrode ($2.3 \times 10^{-11}\,mol\,cm^{-2}$) and then treated with the analyte **3** to yield the ds system. Subsequent interaction of the surface with the **2**-functionalized CdS resulted in the binding of the CdS nanoparticles to the surface. Further alternating interaction of the interface with a solution containing the **1**-functionalized CdS nanoparticles ($1\,mg\,mL^{-1}$) pretreated with **3** (1×10^{-6} M) and with a solution containing **2**-functionalized CdS nanoparticles resulted in an array with a controlled number of CdS nanoparticle generations. The buildup of the DNA-cross-linked CdS nanoparticle array was monitored by microgravimetry with a quartz-crystal microbalance (Figure 2A).

From the frequency changes observed upon the buildup of the first generation of CdS nanoparticles, and knowing their dimensions, we estimate the surface coverage to be about 1.6×10^{12} particles per square centimeter. This value corresponds to around 15% of a densely packed particle layer. The negative charge associated with the nucleic acid functionalized nanoparticles probably prevents the formation of a dense particle configuration. The DNA-cross-linked CdS nanoparticle arrays were also assembled on glass supports by using an aminopropylsiloxane-functionalized glass that was treated with ε-maleimidocaproic *N*-hydroxysuccinimide ester[24, 25] as a base interface for the covalent linkage of **1** and the organization of the nanoparticle systems. Figure 2B shows

[*] I. Willner, F. Patolsky, J. Wasserman
The Institute of Chemistry and
The Farkas Center for Light-Induced Processes
The Hebrew University of Jerusalem
Jerusalem 91904 (Israel)
Fax (+972) 2-6527715
E-mail: willnea@vms.huji.ac.il

[**] This research is supported by The U.S.–Israel Binational Science Foundation. The Max Planck Research Award for International Cooperation (I.W.) is gratefully acknowledged.

Supporting information for this article is available on the WWW under http://www.angewandte.com or from the author.

  1433-7851/01/4010-1861 $ 17.50+.50/0